

## Theoretical study of buckling-based nonlinear transition near a static bifurcation point

Manhee Lee\*

*Department of Physics, Chungbuk National University, Cheongju, Chungbuk 28644, Republic of Korea*

Sangmin An\* and Wonho Jhe†

*Department of Physics and Astronomy, Seoul National University, Gwanak-gu, Seoul 151-747, Republic of Korea*



(Received 27 November 2018; published 1 May 2019)

We theoretically investigate the nonlinear behavior of a buckled tip near the bifurcation point under external stress. We present a mechanical model for the buckled tip and derive the governing equation that describes the “buckling-to-flipping” nonlinear transition of the tip motion. Our minimal mechanistic model fully captures the velocity-dependent flipping phenomena, in which the flip position of the tip varies with the speed of the surface motion, as consistently observed in previous experiments. The present study could be applicable for sensitive detection of directional surface motion such as seismic waves.

DOI: [10.1103/PhysRevE.99.052202](https://doi.org/10.1103/PhysRevE.99.052202)

### I. INTRODUCTION

In nonlinear dynamics, a bifurcation represents a change in the character of the solution as system parameters are varied [1]. Near the bifurcation point, a nonlinear system would be unstable and highly sensitive to external perturbations such as mass loading or force change [2–7]. There have been reported a large number of methods which utilize the bifurcation-enhanced sensitivity in resonant dynamical systems [8–12]. Examples include amplification of small signals near the onset of Duffing bistability [8], bifurcation-based mass detection using piezoelectric microcantilevers [9], and the readout of superconducting quantum bits near a dynamical bifurcation point [11]. While the nonlinearity-assisted sensing is also applicable to nonresonant “static” systems, only a few studies have adopted the “static” bifurcation-based detection [13]. In our previous experimental study, we realized a bifurcation-based sensitive detection of surface acoustic wave by using a static buckled micro-sized tip [14]. We demonstrated that the detection sensitivity in the static system can be enhanced near the bifurcation point. We observed a rapid directional transition between two buckled states, as applying lateral force to the tip.

Here we theoretically investigate the nonlinear transition of “buckling-to-flipping” in the elastically buckled tip. We model the system as a single particle in a double-well potential subject to an external lateral force, which shows a sudden transition in the buckled state as the lateral force applied to the tip is varied. Our model essentially captures the velocity-dependent transition of the state; the transition point alters with the varying rate of the applied force, as consistently observed in previous experiments [14].

### II. THEORY AND RESULT

When an elastic column of tip is axially compressed, buckling takes place at a certain applied load [Fig. 1(a)]. The buckling phenomenon is a bifurcation of equilibrium states of the nonlinear system. For our elastic tip [14], the compressed tip can be in one of the two buckled states; left-buckled or right-buckled [Fig. 1(a)]. A buckled state can be changed by laterally displacing the surface where the buckled tip is pinned. For a left-buckled tip, when the bottom surface moves to the right, the buckled structure is gradually erected and the system suddenly flips into the right-buckled state [Fig. 1(b)]. We note that the initial direction of buckling is preferentially made in a specific direction by slightly tilting the tip to the specific direction, and we can displace the surface to the direction. This allows us to describe the system by the one-dimensional model (Fig. 1).

To derive the governing equation for the “buckling-to-flipping” transition by surface displacement, we model the buckled system as a single particle in a double-well potential, where the particle is attached to a spring and a dashpot, and the spring-dashpot is pulled to the right with a constant velocity  $v$ , as shown in Fig. 1(c). The velocity  $v$  represents the velocity of the lateral motion of the surface [Fig. 1(b)], and the spring and the dashpot denote the system’s elastic and damping constants, respectively. Further, if the system parameter  $v$  is small, the total force exerted on the tip is always balanced, i.e.,  $\ddot{x} \approx 0$ . For this slowly varying system, we obtain the equation of motion,

$$b\dot{x} + kx = kv + bv + F_{\text{ext}}(x), \quad (1)$$

where  $k$  is the elastic coefficient of the spring,  $b$  the damping coefficient of the dashpot, and  $F_{\text{ext}}$  is the force induced by the external potential  $U_{\text{ext}}$ :  $F_{\text{ext}} = -dU_{\text{ext}}/dx$ . To describe the buckled state, we employ a double-well potential for  $U_{\text{ext}}$ ,

$$U_{\text{ext}}(x) = U_0 \frac{16}{a^4} x^2 (x - a)^2, \quad (2)$$

\*These authors contributed equally to this work.

†whjhe@snu.ac.kr

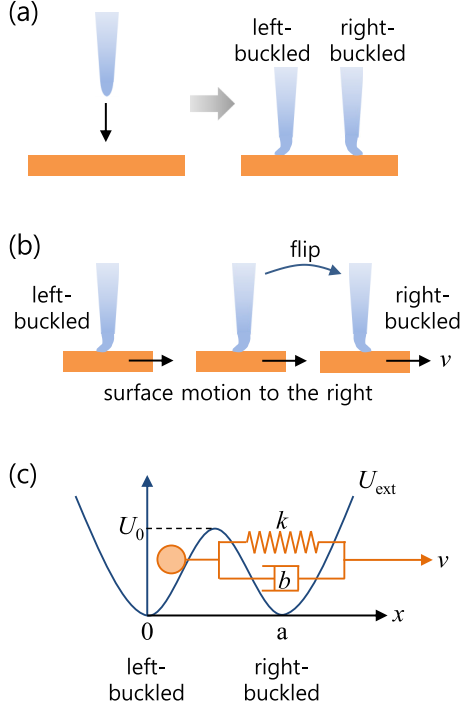


FIG. 1. A buckling of an elastic tip and a mechanistic model for the buckled tip. (a) An elastic tip is buckled under normal compression, and there exist two buckled states, left- and right-buckled states. Refer to Ref. [14] for the experimental realization of the buckling. (b) A buckled state can be suddenly changed by lateral displacement of the surface; here the left-buckled state to the right state, as the bottom surface moves to the right. (c) A mechanistic model of the “buckling-to-flipping” nonlinear transition. A single particle in the left well of a double-well potential, representing the left-buckled tip, can flip to the other state, as the particle is pulled to the right, where the spring and the dashpot exert the elastic and the damping forces on the particle, respectively (see the text for details).

where  $U_0$  indicates the energy barrier between two local minimum states and  $a$  is the width of the two wells. Although there are several parameters in Eqs. (1) and (2), the dimensionless forms of Eqs. (1) and (2) suggest three net parameters,  $a$ ,  $bk^{-1}$ , and  $U_0/(ka^2)$ ;  $a = 67.5$  nm,  $bk^{-1} = 13.5$  ms, and  $U_0/(ka^2) = 5$  were used for comparison with the experiment (see the captions of Figs. 2 and 4 for details).

From the total potential energy of the system, we can qualitatively predict the overall behavior of the tip motion. Let us assume that the tip is initially in left-buckled state at  $t = 0$ . The total potential energy of the system is given by the sum of the double-well potential and the elastic energy associated with the spring constant  $k$  [Fig. 1(c)],

$$U_{\text{tot}} = U_0 \frac{16}{a^4} x^2 (x - a)^2 + \frac{1}{2} k (x - vt)^2. \quad (3)$$

Equation (3) indicates that the elastic energy is gradually stored in the tip structure, as the surface displaces to the right. The depth of the double-well potential represents the energy required to restore the tip structure into the unbuckled structure, and thus the system bifurcates when the elastic energy, stored in the tip by the surface displacement, is comparable to the initial depth of the double-well potential  $U_{\text{ext}}$ . If the tip

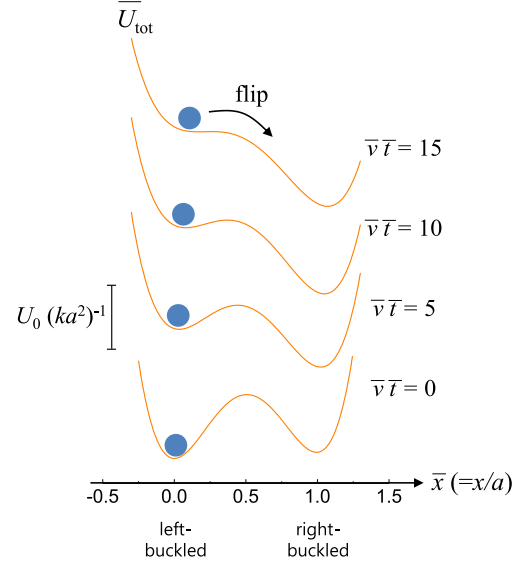


FIG. 2. Total potential energy of the system  $U_{\text{tot}}$  [Eq. (3)], given as the sum of the double-well potential  $U_{\text{ext}}$  and the elastic energy, as a function of the tip position  $\bar{x}$  at different surface displacements  $\bar{v}\bar{t} (= vt/a) = 0.1, 5, 10$ , and  $15$ . The normalized total potential energy is defined as  $\bar{U}_{\text{tot}} \equiv U_{\text{tot}}/(ka^2)$ , the normalized tip position as  $\bar{x} = x/a$ , the normalized time as  $\bar{t} \equiv t/(bk^{-1})$ , and the normalized velocity as  $\bar{v} \equiv v/(ab^{-1}k)$ . Here the potential depth  $U_0 = 5ka^2$  [Eq. (2)] was used for the numerical plot of  $U_{\text{tot}}$ .

initially is in deeply left-buckled, the total potential energy curve [Eq. (3)] at initial left-buckled state exhibits a nearly symmetric shape. As the surface moves to the right, the elastic energy increases, the energy barrier for the tip to reach the other state gradually decreases, and finally the tip flips to the right-buckled state, as described in Fig. 2. By adjusting the surface displacement, one can therefore prepare a buckled tip that is highly sensitive to external disturbances such as acoustic waves, additional mass loading, or environmental changes and can flip its state under the disturbances.

To determine the position of the tip [Fig. 1(b)], or equivalently the position of the particle in the well [Fig. 1(c)], one can solve the equation of motion, Eq. (1). If the system including the tip and the surface [Fig. 1(b)] changes quasistatically, then  $v \approx 0$  and  $\dot{x} \approx 0$ , and Eq. (1) is reduced to the following algebraic equation:

$$kx = kv t + F_{\text{ext}}(x). \quad (4)$$

Here we keep the term  $vt$ , because the system moves slowly for long time and the term  $vt$  would be finite and vary with time. By solving Eq. (4), we obtain the particle position  $\bar{x}$  as a function of the surface displacement  $\bar{v}\bar{t}$  (the black solid curve in Fig. 3). Here the normalized position  $\bar{x}$  is defined as  $x/a$ , the normalized velocity  $\bar{v} \equiv v/(ab^{-1}k)$ , and the normalized time  $\bar{t} \equiv t/(bk^{-1})$ . For the initially left-buckled tip and the surface moving to the right, we find multiple possible positions for the particle at a range of surface positions, as shown in Fig. 3. The multiple valued characteristics lead to the sudden jumps in the position of the tip, indicated by black dashed lines, depending on the direction of the moving tip. For the periodic lateral motion of the surface, this nonlinear

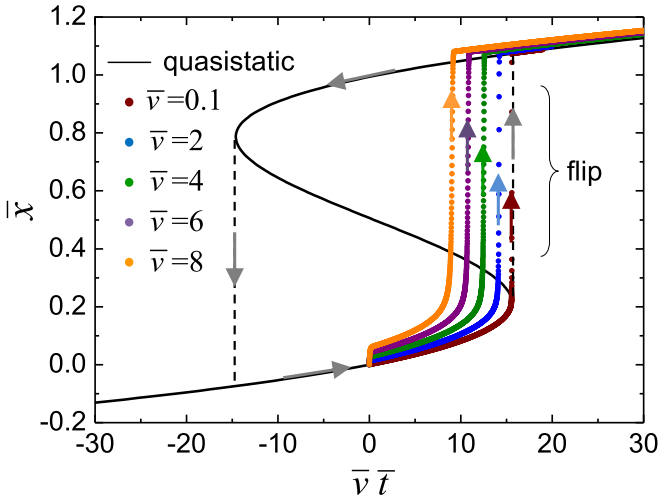


FIG. 3. Velocity-dependent nonlinear transition of the buckling-to-flipping for the buckled tip. For the tip initially in the left-buckled state, the left state flips to the right as the surface displaces to the right by  $\bar{v}\bar{t}$ . The flip point varies with the velocity of the surface motion  $\bar{v}$ , which occurs earlier for larger  $\bar{v}$  (arrow on each dotted curve). The black solid curve shows the tip position  $x$  for quasistatically varying surface displacement  $\bar{v}\bar{t}$  with  $\bar{v} \approx 0$  [Eq. (4)]. The black dashed lines indicate the static bifurcations, and the four gray arrows, two arrows on the solid black curve and two arrows on the dotted black curves, show the direction in which the system evolves between the two states.

response of the tip generates a hysteresis (gray arrows), and the area of the associated force-distance hysteresis equals twice the dissipated energy during one period of the forward-backward flipping processes [14].

The “buckling-to-flipping” transition occurs when the stored energy by the surface displacement is high enough to overcome the initial potential barrier. Here we notice that the damping interaction, indicated by the dashpot in Fig. 1(c), dissipates substantial elastic energy stored in the system after the flip, and thus the buckled tip does not settle back into the initial position of the potential well after the bifurcation.

Experimentally, a parameter, here the surface displacement, that controls nonlinear dynamics of a system is not stationary but varies with time, i.e., is nonadiabatic. The response of the system in such a case would be different from the response of the adiabatic case. To fully describe the experimental system, we now numerically solve Eq. (1) to determine the tip position as varying the surface position underneath the tip. Figure 3 shows the tip position  $\bar{x}$  as a function of the surface displacement  $\bar{v}\bar{t}$  for various surface speeds from 1.5 m/s to 35 m/s. We note that the surface starts to move initially at a given speed  $v$ , and so does the tip, as expected from Eq. (1). This results in the initial slope of the curves in Fig. 3, where the slope at  $t = 0$  increases with the speed  $v$ . Interestingly, we find that the flip position decreases with increasing the speed of the surface motion, as shown in Fig. 3. This velocity-dependent nonlinear transition is a general characteristic behavior when the control parameter, the surface displacement in our case is not stationary but varies continuously and slowly [15]; The bifurcation or loss of stability occurs away from the point at which the static

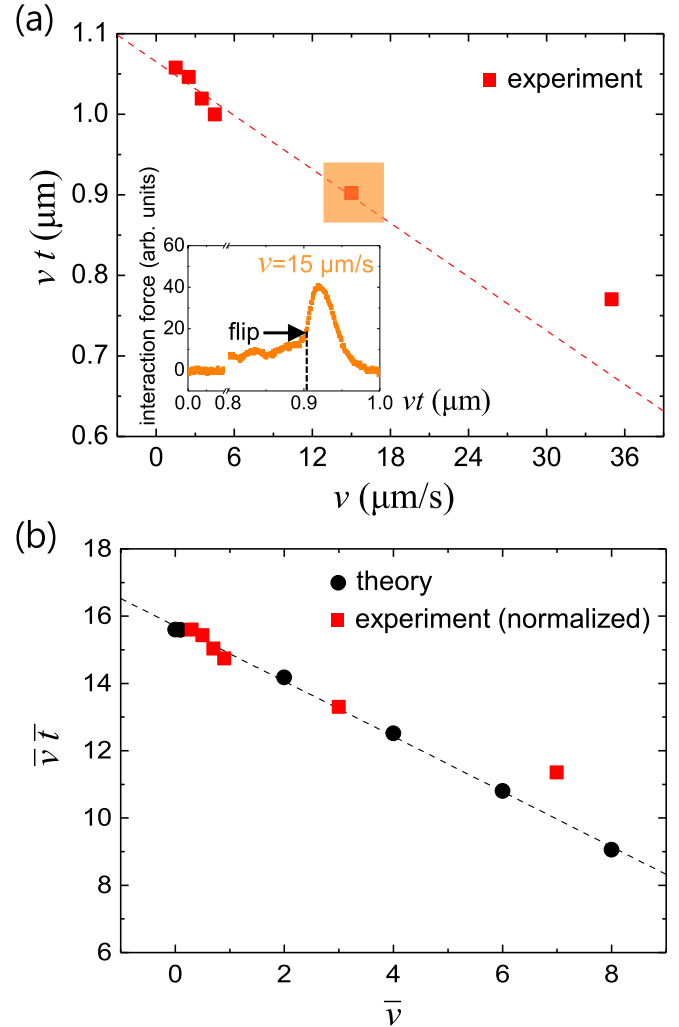


FIG. 4. The flip displacement of the surface,  $\bar{v}\bar{t}$ , as a function of the speed of the surface motion  $\bar{v}$ . (a) The red rectangles are obtained by analyzing our previous experimental data (Fig. 3 in Ref. [14]). For instance, the data plot, the red rectangle in the orange-shaded area (light gray in print version), is obtained from the experimental data shown in the inset. The inset shows the measured interaction force between the buckled tip and the shear sensor, while moving the surface laterally at a speed  $15 \mu\text{m/s}$  (refer to Ref. [14] for details). The transition of the buckled state is reflected by the sudden jump of the interaction force at a specific displacement  $v\bar{t}$ , indicated by the vertical dashed line in the inset. The dashed red curve is the linear fit to the experimental data excluding one outlier at  $v = 35 \mu\text{m/s}$ . (b) The plot of black circles is obtained from the theoretical data shown in Fig. 3 (see the main text for details). The dashed curve is the linear fit to the theoretical data (black circles). For comparison, we have plotted the experimental data (red rectangles) normalized by the constants,  $a = 67.5 \text{ nm}$  and  $bk^{-1} = 13.5 \text{ ms}$ , which were determined by comparing the linear fits, dashed red in (a) and dashed black curves in (b).

bifurcation occurs. This feature was consistently observed in previous experiments [14]. In addition, the earlier flip at higher speed is also predicted from Eq. (1), where the velocity-dependent damping force  $bv$  acts to enhance the tip motion. Provided a buckled tip near the bifurcation point, one, therefore, can realize a surface velocity-dependent detection.

Furthermore, the buckled tip flips its state only if the surface displaces in the specific direction depending on the buckled state. The left-buckled state is changed to the right under only right displacement of the surface, and the left state remains under left displacement. Therefore, the response of the buckled tip is directional.

The displacement of the surface  $vt$ , at which the tip flips, linearly decreases with the speed of the surface motion  $v$ . In previous experiments [14], we qualitatively showed that the flip point decreases with increasing the speed of the surface. Figure 4(a) shows the flip displacement  $vt$  as a function of the speed of the surface  $v$  for an initially left-buckled tip. Those data in Fig. 4(a) were quantitatively obtained by analyzing the experimental data, Fig. 3 in Ref. [14]. For example, the inset shows the interaction force versus the surface displacement, measured by using a sensor of quartz tuning fork, while moving the surface with a speed of  $15 \mu\text{m/s}$ . The flip of the buckled state is then reflected by a sudden jump in the interaction force, so that we can determine the flip displacement of the surface, as indicated by the vertical dashed line in the inset of Fig. 4(a). For comparison, we show the theoretical flip displacement  $\bar{v}\bar{t}$  as a function of the speed  $\bar{v}$ , as shown in Fig. 4(b). Here we obtained the flip displacement  $\bar{v}\bar{t}$  from the transition curve in Fig. 3 in a way that we first find a point in  $\bar{x} - \bar{v}\bar{t}$  plane at which the slope is maximum during the transition (as indicated by colored arrows in Fig. 3), and we define the  $x$  value of the point as the flip transition displacement  $\bar{v}\bar{t}$ . The flip displacement  $\bar{v}\bar{t}$  decreases with increasing the speed  $\bar{v}$  [black circles in Fig. 4(b)], as expected in Fig. 3. Moreover, we find a linear dependence of the flip displacement on the speed in Fig. 4(b), where the dashed black curve is the linear fit to the theoretical data (black circles). This linearity is consistently found in experimental results (red rectangles), as shown in Fig. 4(b).

### III. CONCLUSION

In conclusion, the bifurcation-based detection method using nonresonant static system, here the buckled tip, offers a strategy to enhance the detection sensitivity that is very often limited in linear systems. With a linear static system, e.g., a microcantilever, one can detect external force by measuring the cantilever displacement, which is given by the force divided by the cantilever's stiffness. Since a cantilever with lower stiffness allows higher displacement for a given force, one has to prepare a cantilever with desired stiffness, which is a characteristic constant of the tip. On the other hand, we can alter the detection sensitivity of the buckled tip on demand, by changing the energy barrier to overcome via the surface displacement. Interestingly, a seismoscope from ancient China [16] adopted such a bifurcation-based detection scheme, in which a lateral disturbance would flip small balls inside the system out of its potential well, and the direction of the surface wave could be determined. Our results would be applicable to develop a new type of mechanical sensors of surface acoustic waves, such as seismometers [17,18].

### ACKNOWLEDGMENTS

This work was supported by a National Research Foundation of Korea (NRF) grant funded by the Korean government (Ministry of Science & Information and Communication Technology) (Grants No. 2017R1C1B5076655, and No. 2016R1A3B1908660), a research grant of Chungbuk National University in 2017, and the Basic Science Research Program through the NRF funded by the Ministry of Education (Grant No. 2017R1A6A3A11033301).

- 
- [1] S. H. Strogatz, *Nonlinear Dynamics and Chaos: with Applications to Physics, Biology Chemistry and Engineering* (Westview Press, Boulder, 2001).
  - [2] K. P. Singh, R. Kapri, and S. Sinha, Scalable ultra-sensitive detection of heterogeneity via coupled bistable dynamics, *Europhys. Lett.* **98**, 60004 (2012).
  - [3] V. Kohar, A. Choudhary, K. P. Singh, and S. Sinha, Verification of scalable ultra-sensitive detection of heterogeneity in an electronic circuit, *Eur. Phys. J. Special Topics* **222**, 721 (2013).
  - [4] M. I. Dykman, D. G. Luchinsky, R. Mannella, P. V. E. McClintock, N. D. Stein, and N. G. Stocks, Supernarrow spectral peaks and high-frequency stochastic resonance in systems with coexisting periodic attractors, *Phys. Rev. E* **49**, 1198 (1994).
  - [5] H. Krömmner, A. Erbe, A. Tilke, S. Manus, and R. Blick, Nanomechanical resonators operating as charge detectors in the nonlinear regime, *Europhys. Lett.* **50**, 101 (2000).
  - [6] S. Savel'ev, A. Rakhmanov, and F. Nori, Nonlinear amplifier and frequency shifter using a tunable periodic drive, *Phys. Rev. E* **72**, 056136 (2005).
  - [7] H. B. Chan and C. Stambaugh, Fluctuation-enhanced frequency mixing in a nonlinear micromechanical oscillator, *Phys. Rev. B* **73**, 224301 (2006).
  - [8] R. Almqvist, S. Zaitsev, O. Shtempluck, and E. Buks, High intermodulation gain in a micromechanical Duffing resonator, *Appl. Phys. Lett.* **88**, 213509 (2006).
  - [9] V. Kumar *et al.*, Bifurcation-based mass sensing using piezoelectrically-actuated microcantilevers, *Appl. Phys. Lett.* **98**, 153510 (2011).
  - [10] E. Buks and B. Yurke, Mass detection with a nonlinear nanomechanical resonator, *Phys. Rev. E* **74**, 046619 (2006).
  - [11] I. Siddiqi, R. Vijay, F. Pierre, C. M. Wilson, M. Metcalfe, C. Rigetti, L. Frunzio, and M. H. Devoret, RF-Driven Josephson Bifurcation Amplifier for Quantum Measurement, *Phys. Rev. Lett.* **93**, 207002 (2004).
  - [12] A. N. Cleland, Thermomechanical noise limits on parametric sensing with nanomechanical resonators, *New J. Phys.* **7**, 235 (2005).
  - [13] C. Yu, Z. Wang, H. Yu, and H. Jiang, A stretchable temperature sensor based on elastically buckled thin film devices on elastomeric substrates, *Appl. Phys. Lett.* **95**, 141912 (2009).
  - [14] S. An, B. Kim, S. Kwon, G. Moon, M. Lee, and W. Jhe, Bifurcation-enhanced ultrahigh sensitivity of a buckled cantilever, *Proc. Natl. Acad. Sci. USA* **101**, 2884 (2018).

- [15] A. Raman, A. K. Bajaj, and P. Davies, On the slow transition across instabilities in nonlinear dissipative systems, *J. Sound Vib.* **192**, 835 (1996).
- [16] K.-H. Hsiao and H.-S. Yan, Structural synthesis of Zhang Heng's seismoscope with cam-linkage mechanisms, *J. Adv. Mech. Des. Syst.* **3**, 179 (2009).
- [17] J. Havskov and G. Alguacil, *Instrumentation in Earthquake Seismology* (Springer, New York, 2004).
- [18] D. Stuart-Watson and J. Tapson, Simple force balance accelerometer/seismometer based on a tuning fork displacement sensor, *Rev. Sci. Instrum.* **75**, 3045 (2004).